2022 11th International Conference on Control, Automation and Information Sciences (ICCAIS) | 978-1-6654-5248-9/22/$31.00 ©2022 IEEE | DOI: 10.1109/ICCAIS56082.2022.9990549

An Adaptive Multi-Sensor Generalised Labelled Multi-Bernoulli Filter for Linear Gaussian Models

Tran Thien Dat Nguyen*, Cong-Thanh Do†, and Hoa Van Nguyen‡
*‡*School of Electrical Engineering, Computing and Mathematical Sciences, Curtin University, Australia*
†*Faculty of Mechanical, Electrical, and Electronic Technology, Thai Nguyen University of Technology, Vietnam*
* t.nguyen1@curtin.edu.au, † thanhdc@tnu.edu.vn, ‡ hoa.v.nguyen@curtin.edu.au.

Abstract—**Recent development of the multi-sensor generalised labelled multi-Bernoulli (MS-GLMB) tracking algorithm allows joint estimation of target trajectories adjunct to clutter rate and detection probability. Nevertheless, it requires prior knowledge of new birth target distribution which might not be available in certain tracking scenarios. Conversely, another algorithm has been proposed to handle unknown birth statistics using multi-sensor measurement and a Gibbs sampler, but not be able to estimate clutter rate and detection probability. In this paper, we propose a multi-sensor multi-target tracking algorithm to handle unknown clutter rate, detection profile, and statistics of new birth targets. Our algorithm assumes linear Gaussian property on the dynamic and measurement models for closed-form analytic computation. Experiment with a 3-D tracking scenario demonstrates the robustness of our algorithm.**

I. Introduction

Reliable clutter statistics and detection profile are important for accurate tracking results. Common practice assumes this information is available to the filters, which can be from prior knowledge, learnt from similar scenarios, or parameter fine-tuning. However, learning or tuning for this information could be difficult and tedious. In random finite set (RFS) tracking paradigm, estimation of clutter statistics and detection probability can be performed by modelling clutter as a different type of targets and augmenting the detection probability to the target state-space. Methods based on this approach have demonstrated their robust tracking capability in [1]–[8].

Birth statistical information is also crucial for tracking. This information is the prior knowledge of where new targets appear in the tracking region. In practice, birth statistic is assumed to be known beforehand and supplied to the filters to perform tracking. Nevertheless, in many applications, new births could appear anywhere in the target tracking state-space. Hence, the birth statistic is uninformative, which degrades the performance of the filters due to high uncertainty. One approach is to use partially uniform birth model [9] while another is to use birth distribution that is constructed from the past measurements [10], [11]. The latter approach is straightforward in single-sensor tracking where each new birth target can only generate at most one measurement. Nevertheless, in multi-sensor tracking, a new birth target can be detected by multiple sensors. Hence, the task of generating birth statistic is much more difficult. Recently, a multi-sensor adaptive birth solution has recently been proposed in [12]. It uses a Gibbs sampler to generate highly probable components of the birth distribution. These components are constructed using combinations of measurements from different sensors.

This work is supported by the Australian Research Council under Linkage project LP200301507, and the Defence Science Centre Collaborative Research Grant in 2020.

In this work, we propose an adaptive filtering algorithm that can effectively perform multi-sensor multi-target tracking with unknown detection profile, clutter and birth statistics altogether. We base our solution on the robust MS-GLMB filter [13] which consists of a bank of robust cardinalised probability hypothesis density (CPHD) filters [3] for clutter estimation and a MS-GLMB filter [14] to estimate detection probability and target states. The method in [12] is used to construct new birth distribution from multi-sensor measurements. Our algorithm assumes linear Gaussian property on the dynamic and measurement models for closed-form analytic computation.

The structure of our paper is as follow. In Section II, we provide discussions on the GLMB-based filters and the robust tracking approaches. Section III presents the detailed formulation of our solution. In Section IV, we conduct a numerical study to show the effectiveness of our approach. Finally, Section V concludes the paper.

II. Background

Early works on RFS tracking filters (e.g., the probability hypothesis density (PHD) or CPHD filter) did not include target identities implicitly in their formulations. Hence, in principle, they are not able to estimate target trajectories. The first systematic formulation of the labelling concept for RFS tracking filters was introduced by Vo and Vo [15]. This formulation led to the invention of the GLMB filter [16], [17] which is a tractable exact closed-form Bayes filter for multi-target tracking [18]. Notably, the filter has been implemented to track over one million targets with only off-the-shelve computing hardware [19]. Further, a GLMB filter that can handle multi-sensor measurements has been proposed in [14]. This algorithm is readily applicable to problems with a large number of measurements since its complexity is linear in the total number of measurements from all sensors. An GLMB-based algorithm proposed in [20] is able to perform multi-target estimation over multiple scans, which is recently developed to also handle multi-sensor measurement [21]. In practice, GLMB-based filters have been applied to solve problems ranging from biological cell tracking [22]–[24], control/automation [25]–[29], crowd surveillance [6], [30]–[35] to space debris tracking [36]–[38].

For single-sensor tracking, Mahler et al. proposed methods to estimate clutter rate and detection probability of targets using the CPHD or PHD filter in [3]. These filters render low complexity due to their formulations that do not require solving the data association problem. Similar approach based on the multi-Bernoulli filter has also been proposed in [4]. Conversely, detection probability and clutter statistics can also be estimated by the GLMB filter as proposed in [6]. However, the complexity naturally increases since clutter needs to be included in the data association scheme. In terms of accuracy and complexity balance, the bootstrapping algorithms which combine the first order approximation filters (i.e., PHD or CPHD filter) and the labelled RFS filters (i.e., GLMB filter) are promising robust tracking solutions. In [8], at each time step, a robust CPHD filter is used estimate the clutter rate and average detection probability, which are then bootstrapped into the GLMB filter for multi-target state estimation. This bootstrapping method has also been applied to multi-sensor tracking in [13]. Although, in [13], target detection probability is estimated by the MS-GLMB filter (by augmenting target detection probability to the state-space).

When useful birth statistics are not available, uniform birth distribution can be assumed. However, such birth model leads to high uncertainty, which could degrade the filter performance. In practice, current measurements are used to construct the birth distribution at the next time step [10], [11]. In single-sensor tracking, this measurement-driven approach is straight forward. Nonetheless, in multi-sensor tracking, measurement combinations from different sensors need to be considered. A recent method in [12] proposed using Gibbs sampler to select significant components of the new birth distribution. Especially, calculations of the conditional sampling distribution and target state distribution can be done analytically if linear Gaussian dynamic and measurement models are assumed.

III. An Adaptive MS-GLMB Filter

A. Filter Schematic

The schematic of our filter for one time frame is given in Fig. 1. This filter shares similar structure to the robust MS-GLMB filter in [13] with an additional Gibbs sampler module to generate multi-target birth distribution from the posterior GLMB density and the multi-sensor measurement set.

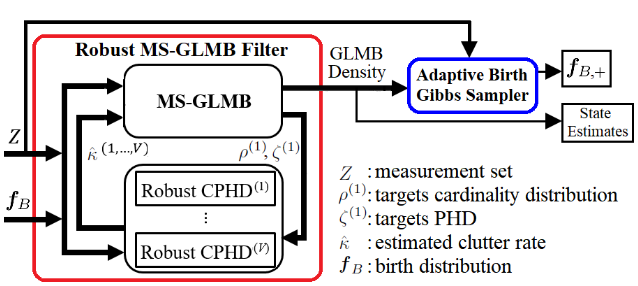

Fig. 1. Schematic of the proposed adaptive multi-sensor filter.

B. Notations

We denote the set exponential as $[h(\cdot)]^X = \prod_{x\in X} h(x)$, and the inner product as $\langle f, g\rangle = \int f(x)g(x)dx$. The generalisation of the Kronecker delta and set inclusion functions are defined respectively as

$$\delta_Y(X)=\begin{cases}1, & X=Y\\ 0, & X\neq Y\end{cases} \text{ and } 1_Y(X)=\begin{cases}1, & X\subseteq Y\\ 0, & otherwise\end{cases}. \quad (1)$$

We use bold upper case symbol (e.g., $\boldsymbol{X}$) to denote the labelled set of objects, and bolded lower case $\boldsymbol{x}$ for a labelled object. We let $\mathcal{L}$ denote the label extraction function, i.e., $\mathcal{L}(\boldsymbol{x}) = \ell$ for $\boldsymbol{x} = (x, \ell)$ with $x \in \mathbb{X}$ and $\ell \in \mathbb{L}$ ($\mathbb{X}$ is target state-space and $\mathbb{L}$ is a discrete label space), and $\mathcal{F}(\mathbf{X})$ denote sets of finite subsets of $\boldsymbol{X}$. The "+" sign denotes the next time step.

C. The Robust MS-GLMB Filter

A GLMB density can be written as [15]

$$\boldsymbol{\pi}(\boldsymbol{X}) = \Delta(\boldsymbol{X}) \sum_{(I,\xi)\in\mathcal{F}(\mathbb{L})\times\Xi} \omega^{(I,\xi)}\delta_I(\mathcal{L}(\boldsymbol{X}))\left[p^{(\xi)}\right]^{\boldsymbol{X}}, \quad (2)$$

where I represents a set of labels, $\xi \in \Xi$ is a history of association maps up to time k, and $\Delta(\boldsymbol{X})$ equals 1 if $|\boldsymbol{X}| = |\mathcal{L}(\boldsymbol{X})|$ and 0 otherwise. Each $p^{(\xi)}(\cdot, \ell)$ represents the distribution of a target state with $\int p^{(\xi)}(x,\ell)\,dx = 1$, and the non-negative weights $\omega^{(I,\xi)}$ satisfy,

$$\sum_{I\in\mathcal{F}(\mathbb{L})}\sum_{\xi\in\Xi}\omega^{(I,\xi)} = 1. \quad (3)$$

In the robust MS-GLMB filter, the target detection probability is also augmented to the state-space. Hence, each labelled single-target state is represented by $\boldsymbol{x} = (x, \alpha, \ell)$ where x is the kinematic state of the target, $\alpha = [\alpha_1, ..., \alpha_V] \in [0,1]^V$ is the detection probability of the target on V sensors (assuming there are V sensors in the observation system), and ℓ is its distinct label. We assume the probability density on the kinematic state of the target and the detection probability are independent, i.e., $p^{(\xi)}(x,\alpha,\ell) = p^{(\xi)}(x,\ell)\prod_{s=1}^{V} p^{(\xi)}(\alpha_s)$. The set of measurements observed from a sensor s is denoted as $Z^{(s)} = z^{(s)}_{1:|Z^{(s)}|} \in \mathbb{Z}$. Given the single-sensor likelihood can be written as [13]

$$\psi^{(s,j)}_{\{z_{1:|Z^{(s)}|}\}}(x,\alpha,\ell) = \begin{cases}\frac{\alpha_s g^{(s)}(z_j|(x,\ell))}{\hat{\kappa}^{(s)}(z_j)}, & j = 1:|Z^{(s)}|\\ 1-\alpha_s, & j=0.\end{cases}, \quad (4)$$

where $g^{(s)}$ is the single-target likelihood of the sensor s and $\hat{\kappa}^{(s)}$ is the clutter rate estimated by a robust CPHD filter, following [14], we make the following abbreviations:

$$Z \triangleq \left(Z^{(1)},\dots,Z^{(V)}\right); \theta \triangleq \left(\theta^{(1)},\dots,\theta^{(V)}\right); \quad (5)$$

$$\Theta(I) \triangleq \Theta^{(1)}(I)\times\cdots\times\Theta^{(V)}(I); \Theta \triangleq \Theta^{(1)}\times\cdots\times\Theta^{(V)}; \quad (6)$$

$$1_{\Theta(I)}(\theta) \triangleq \prod_{s=1}^{V} 1_{\Theta^{(s)}(I)}\left(\theta^{(s)}\right); \quad (7)$$

$$\psi_Z^{(j^{(1)},\dots,j^{(V)})} \triangleq \prod_{s=1}^{V}\psi_Z^{(s,j^{(s)})}(x,\alpha,\ell); \quad (8)$$

where $\theta^{(s)} \in \Theta^{(s)}$ is a 1-1 positive map $\theta^{(s)}:\mathbb{L}\to\{0:|Z^{(s)}|\}$.

For a prior multi-target density given in (2), the filtering density given a set of multi-sensor measurement Z_+ is [13]

$$\boldsymbol{\pi}_+\left(\boldsymbol{X}_+|Z_+\right) \propto \Delta\left(\boldsymbol{X}_+\right) \sum_{I,\xi,I_+,\theta_+} \omega^{(I,\xi)}\omega_{Z_+}^{(I,\xi,I_+,\theta_+)}\delta_{I_+}\left[\mathcal{L}\left(\boldsymbol{X}_+\right)\right]\left[p_{Z_+}^{(\xi,\theta_+)}\right]^{\boldsymbol{X}_+}, \quad (9)$$

where $I \in \mathcal{F}(\mathbb{L}), \xi \in \Xi, I_+ \in \mathcal{F}(\mathbb{L}_+), \theta_+ \in \Theta_+(I_+)$,

$$\omega_{Z_+}^{(I,\xi,I_+,\theta_+)} = 1_{\Theta_+(I_+)}(\theta_+)\left[1-\bar{P}_S^{(\xi)}\right]^{I-I_+}\left[\bar{P}_S^{(\xi)}\right]^{I\cap I_+} \times\left[1-r_{B,+}\right]^{\mathbb{B}_+-I_+} r_{B,+}^{\mathbb{B}_+\cap I_+}\left[\bar{\psi}_{Z_+}^{(\xi,\theta_+)}\right]^{I_+}, \quad (10)$$

$$\bar{P}_S^{(\xi)}(\ell) = \left\langle p^{(\xi)}(\cdot,\ell), P_S(\cdot,\ell)\right\rangle, \quad (11)$$

$$\bar{\psi}_{Z_+}^{(\xi,\theta_+)}(\ell) = \int \bar{p}_+^{(\xi)}(x,\ell)\prod_{s=1}^{V} p^{(\xi)}(\alpha_s) \times\psi_{Z_+}^{(\theta_+(\ell))}(x,\alpha,\ell)\,dx d\alpha_{1:V}, \quad (12)$$

$$p_S(x,\alpha,\ell) = \int P_S(\zeta,\ell) f_{S+}(x|\zeta,\ell)p^{(\xi)}(\zeta,\ell)\,d\zeta \times\prod_{s=1}^{V}\int p^{(\xi)}(\bar{\alpha}_s)f_{\Delta+}^{(s)}(\alpha_s|\bar{\alpha}_s)d\bar{\alpha}_s, \quad (13)$$

$$\bar{p}_+^{(\xi)}(x,\alpha,\ell) = 1_{\mathbb{L}}(\ell)\frac{p_S(x,\alpha,\ell)}{\bar{P}_S^{(\xi)}(\ell)} + 1_{\mathbb{B}_+}(\ell)\,p_{B,+}(x,\ell), \quad (14)$$

$$p_{Z_+}^{(\xi,\theta_+)}(x,\alpha,\ell) = \frac{\bar{p}_+^{(\xi)}(x,\alpha,\ell)\,\psi_{Z_+}^{(\theta_+(\ell))}(x,\alpha,\ell)}{\bar{\psi}_{Z_+}^{(\xi,\theta_+)}(\ell)}, \quad (15)$$

P_S is the survival probability of a target, $f_{S,+}$ is the single-target state transition density, $f_{\Delta+}^{(s)}$ is the transition density of the detection probability of target on a sensor s, $\mathbb{B}_+$ is the space of new birth labels, $r_{B,+}$ is the existence probability of a new birth and $p_{B,+}$ is the distribution of its state. For tractability, high-weight components (I,ξ,I_+,θ_+) are sampled using a Gibbs sampler. For efficiency, we use the sub-optimal Gibbs sampler presented in Algorithm 2 of [14]. Note that, as seen in Fig. 1, in addition to estimating the detection probability, the robust MS-GLMB filter also estimates the clutter rate of each sensor from a bank of CPHD filters, which differs it from the the standard MS-GLMB filter [14].

D. The Adaptive Birth Gibbs Sampler

For compact notation, we introduce the following definitions. For a sensor s, we define $\mathbb{J}^{(s)} = \{1,....,\left|Z^{(s)}\right|\}$ such that each $j^{(s)}$ is a unique index of the enumerate measurement set $Z^{(s)}$, and $\mathbb{J}_0^{(s)} = \{0\}\cup\mathbb{J}^{(s)}$ with 0 index denotes the miss-detection. We abbreviate $\mathbb{J}_0 \triangleq \mathbb{J}_0^{(1)}\times\cdots\times\mathbb{J}_0^{(V)}$ and $J \triangleq j^{(1)}\times\cdots\times j^{(V)}$ [12] (we refer to J as a *multi-sensor measurement index tuple*).

Note that the filtering formulation presented in previous subsection assumes an labelled multi-Bernoulli (LMB) birth model where each hypothesized track has an existence probability $r_{B,+}$ and a state distribution $p_{B,+}$. In this context, this LMB birth distribution can be written as

$$\boldsymbol{f}_{B,+} = \left\{\left(r_{B,+}(\ell_+), p_{B,+}(x_+,\alpha_+,\ell_+|Z_J)\right)\right\}_{\ell_+\in\mathbb{B}_+}. \quad (16)$$

The space of Z_J is large since it contains the combination of measurements on different sensors and the miss-detection. Hence, our objective is to sample for the components of $\boldsymbol{f}_{B,+}$ with high existence probability $r_{B,+}$. Note that for $p_{B,+}(x_+,\alpha_+,\ell_+) = p_{B,+}(x_+,\ell_+)\prod_{s=1}^{V} p_{B,+}(\alpha_{s,+})$, assuming we have the prior knowledge on $p_{B,+}(\alpha_{s,+})$, the remaining task is to compute $p_{B,+}(x_+,\ell_+)$. The rest of this subsection is dedicated to show how to construct the sampling distribution and to compute the resulting $r_{B,+}$ and $p_{B,+}(x_+,\ell_+)$. More details can be found in [12].

Given the filtering GLMB density (9), the association probability of a measurement $z_{j^{(s)},+}^{(s)}$ (the probability that this measurement has already been assigned to a target) is

$$r_A(j^{(s)}) \propto \sum_{I,\xi,I_+,\theta_+} 1_{\theta_+^{(s)}}(j^{(s)})\omega^{(I,\xi)}\omega_{Z_+}^{(I,\xi,I_+,\theta_+)}. \quad (17)$$

Conventionally, we set $r_A(0) = 0$ [12]. The unassociation probability of a multi-sensor measurement index tuple J_+ is

$$r_U \propto \left[1-r_A\right]^{J_+}. \quad (18)$$

Conversely, the spatial distribution of a new birth with label ℓ_+ (at the current time step) due to measurement tuple Z_J can be written via Bayes rule as [12]

$$p_{B,+}(x,\ell_+|Z_J) = \frac{p_B(x,\ell_+)\psi_Z^{(J)}(x,\ell_+)}{\bar{\psi}_Z^{(J)}(\ell_+)}, \quad (19)$$

where $\bar{\psi}_Z^{(J)}(\ell_+) = \langle p_B(\cdot,\ell_+), \psi_Z^{(J)}(\cdot,\ell_+)\rangle$. The birth distribution at the next time step is then

$$p_{B,+}(x_+,\ell_+|Z_J) = \int f_+(x_+|x,\ell_+)p_{B,+}(x,\ell_+|Z_J)dx. \quad (20)$$

The existence probability of a birth that is generated by a multi-sensor measurement index tuple J is written as

$$r_{B,+}(\ell_+) = \min\left(r_{B,max}, \lambda_{B,+}\times\hat{r}_{B,+}^{(J)}(\ell_+)\right), \quad (21)$$

where $\lambda_{B,+}$ is the number of expected births and [12]

$$\hat{r}_{B,+}^{(J)}(\ell_+) = \frac{r_U(J)\bar{\psi}_Z^{(J)}(\ell_+)}{\sum_{J'\in\mathbb{J}_0} r_U(J')\bar{\psi}_Z^{(J')}(\ell_+)}. \quad (22)$$

Since we are interested in sampling for the components of $\boldsymbol{f}_{B,+}$ with high $r_{B,+}(\ell_+)$, we need to sample for $\ell_+\in\mathbb{B}_+$ from some $p(\ell_+)$ such that

$$p(\ell_+) \propto r_{B,+}(\ell_+) \propto \hat{r}_{B,+}(\ell_+) \propto r_U(J)\bar{\psi}_Z^{(J)}. \quad (23)$$

According to Theorem V.1 in [12], for $J^{(-s)} = (j^{(1)},...,j^{(s-1)},j^{(s+1)},...,j^{(V)})$, we have

$$p(\ell_+) \propto p(j^{(s)}|J^{(-s)}) \propto (1-r_A(j^{(s)}))\bar{\psi}_Z^{(J)}(\ell_+). \quad (24)$$

Sampling from the conditional distribution $p(j^{(s)}|J^{(-s)})$ is straight forward using a Gibbs sampler.

By assuming linear Gaussian kinematic measurement model, i.e., $g^{(s)}(z|(x,\ell)) = \mathcal{N}(z,H^{(s)}x,R^{(s)})$, and a Gaussian birth kinematic prior distribution, i.e., $p_B(x,\ell_+) = \mathcal{N}(x,\mu_0,P_0)$, the conditional distribution $p(j^{(s)}|J^{(-s)})$ can be computed in closed-form as [12]

$$p(j^{(s)}|J^{(-s)}) \propto \begin{cases} (1-P_D^{(s)})\det(M_{J(-s)})^{-\frac{1}{2}}\Phi_{J(-s)}, & j^{(s)}=0 \\ \left[(2\pi)^{n_z^{(s)}}\det(M_J)\det(R^{(s)})\right]^{-\frac{1}{2}} & \\ \times(1-r_A(j^{(s)}))\frac{\bar{P}_D^{(s)}}{\hat{\kappa}^{(s)}(z_{j^{(s)}}^{(s)})}, & j^{(s)}>0 \end{cases} \quad (25)$$

where $n_z^{(s)}$ is the measurement dimension, $\bar{P}_D^{(s)}$ is the average detection probability computed from the filtering density (9), $\hat{\kappa}^{(s)}$ is the estimated clutter rate of the s^{th} sensor, and

$$\Phi_J = \exp\left(-\frac{1}{2}(c_J - b_J^T M_J^{-1} b_J)\right), \quad (26)$$

$$M_J = P_0^{-1} + \sum_{s'=1,j^{(s')}>0}^{V} \left(H^{(s')}\right)^T \left(R^{(s')}\right)^{-1} H^{(s')}, \quad (27)$$

$$b_J = P_0^{-1}\mu_0 + \sum_{s'=1,j^{(s')}>0}^{V} \left(H^{(s')}\right)^T \left(R^{(s')}\right)^{-1} z_{j^{(s')}}^{(s')}, \quad (28)$$

$$c_J = \mu_0^T P_0^{-1}\mu_0 + \sum_{s'=1,j^{(s')}>0}^{V} \left(z_{j^{(s')}}^{(s')}\right)^T \left(R^{(s')}\right)^{-1} z_{j^{(s')}}^{(s')}. \quad (29)$$

Further, assuming the linear Gaussian kinematic state transition model, i.e., $f(x_+|x) = \mathcal{N}(x_+, Fx, Q)$, the component of the birth distribution is given as

$$p_{B,+}(x_+, \ell_+|Z_J) = \mathcal{N}(x; \mu_B, P_B), \quad (30)$$
$$\mu_B = FM_J^{-1}b_J \text{ and } P_B = FM_J^{-1}F^T + Q.$$

Given the closed-form expression of the weight $\bar{\psi}_{Z_+}^{(J)}(\ell_+)$, i.e.,

$$\bar{\psi}_{Z_+}^{(J)}(\ell_+) = \left[\det(P_0)\det(M_J)\prod_{s'=1}^{V}(2\pi)^{n_z^{(s')}}\det(R^{(s')})\right]^{-\frac{1}{2}}$$
$$\times \left[\prod_{s'=1,j^{(s')}>0}^{V} 1-P_D^{(s)}\right]\left[\prod_{s'=1,j^{(s')}>0}^{V} \frac{P_D^{(s')}}{\kappa^{(s')}(z_{j^{(s')}}^{(s')})}\right]\Phi_J, \quad (31)$$

$r_{B,+}(\ell_+)$ can be computed using (21).

IV. Experiment

In this experiment, we set up a tracking scenario with 12 distinct targets moving in a 3-D space as in [21]. There are 3, 3, 2, 2, and 2 targets appear at time 1, 20, 40, 60, and 80, respectively. The tracking duration is 100 time steps (1s per time step). For the first 50 time steps, the true detection probability is 0.8 and the true clutter rate is 70 (for tracking scenarios with low detection threshold). For the remaining time steps, they are 0.3 and 20 (for tracking scenarios with high detection threshold), respectively. The targets move with constant velocity model. Hence, the transition density of the kinematic state is $f(x_+|x) = \mathcal{N}(x_+, Fx, Q)$ with

$$F = \mathbf{I}_3 \otimes \begin{bmatrix} 1 & \Delta \\ 0 & 1 \end{bmatrix}, Q = \sigma_a^2 \mathbf{I}_3 \otimes \begin{bmatrix} \frac{\Delta^4}{4} & \frac{\Delta^3}{2} \\ \frac{\Delta^3}{2} & \Delta^2 \end{bmatrix}, \quad (32)$$

$\mathbf{I}_n$ is the n-D identity matrix, and $\otimes$ denotes the Kronecker multiplication. We set $\sigma_a = 5\ m/s^2$ and $\Delta = 1s$ in this experiment. The detection probability is modelled by beta distributions. The initial parameters of the distributions are chosen such that we have an average detection probability of 0.5 for each track. There are four 3-D positional sensors in the system with each has the surveillance region of $[-1500m, 1500m]^3$ (where $\mathbb{A}^n \triangleq \underbrace{\mathbb{A}\times\ldots\times\mathbb{A}}_{n \text{ times}}$ for an arbitrary space $\mathbb{A}$). The likelihood function for each sensor is given as

$$g^{(s)}(z|(x,\ell)) = \mathcal{N}(z, H^{(s)}x, R^{(s)}), \quad (33)$$

where $H^{(s)} = \mathbf{I}_3 \otimes \begin{bmatrix} 1 & 0 \end{bmatrix}$ and $R^{(s)} = \text{diag}(\begin{bmatrix} 20^2 & 20^2 & 20^2 \end{bmatrix})$.

For computing the measurement-driven birth distribution, we set $r_{B,max} = 0.03$ with the number of expected birth for each time step, $\lambda_{B,+}$, is 1. The prior kinematic distribution of birth is Gaussian with mean $\mu_0 = \begin{bmatrix} 0 & 0 & 0 & 0 & 0 & 0 \end{bmatrix}^T$ and covariance $P_0 = \text{diag}(\begin{bmatrix} 2000^2 & 50^2 & 2000^2 & 50^2 & 2000^2 & 50^2 \end{bmatrix})$. For the first time step, the average detection probability $\bar{P}_D^{(s)}$ for a sensor s is set to 0.5 and $\hat{\kappa}^{(s)} = 5/\mathscr{V}^{(s)}$ with $\mathscr{V}^{(s)}$ is the volume of the surveillance region. At each time step, we sample 10,000 GLMB components using the sub-optimal Gibbs sampler. For measurement-driven birth, we generate 1,000 samples of new birth components. We discard birth components that are generated by multi-sensor measurement tuples with more than 1 miss-detection. In Fig. 2, we show the true and estimated tracks from our method in 1 Monte Carlo (MC) run. We use the sub-optimal estimator proposed in [15] to extract track estimates although trajectory smoothing can also be further applied [20].

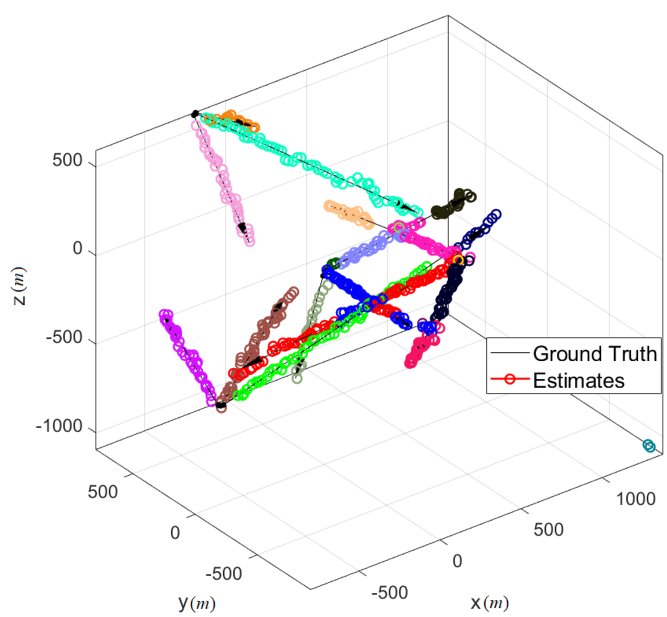

Fig. 2. Ground truth and estimated tracks from our method.

We compare our algorithm with others including the adaptive birth AB-MS-GLMB [12], robust R-MS-GLMB [13], and MS-GLMB [14]. For the filters that require prior information on the detection probability and clutter rate (i.e., AB-MS-GLMB and MS-GLMB), we supply them with the mean values (i.e., detection probability of 0.55 and clutter rate of 45). For the filters that require prior knowledge on the birth statistics (i.e., R-MS-GLMB and MS-GLMB), we use a uniform birth distribution with each component is a Gaussian density with mean $\mu_{B,+} \in [\{-1000, -500, ..., 1000\} \times \{0\}]^3$ and covariance matrix $P_{B,+} = \text{diag}([\ 100^2 \quad 10^2 \quad 100^2 \quad 10^2 \quad 100^2 \quad 10^2\ ])$. For comparable computation time with other filters, we only randomly select 50 birth components at each time step.

All algorithms are tested for 100 MC runs. To evaluate the performance, we use the OSPA$^{(2)}$ metric [19] to measure the distances (errors) between the estimates and ground truth sets of tracks (see [39] for a detailed analysis on the performance criteria). We set the metric cut-off to 100 m and order to 2 with the window length of 10. The errors for all algorithms are presented in Fig. 3. We show the error together with its cardinality and localisation components for better insight. In Fig. 4, we present the estimated cardinality for each time step. We also plot the estimated detection probability and clutter rate provided by our method and the R-MS-GLMB filter in Fig. 5. The results are the mean values over all MC runs with the thin broken lines show one standard deviation bounds.

Fig. 3 shows errors of the proposed method and the AB-MS-GLMB filter are similar but lower than others for the first half tracking duration due to the more accurate track initiation. Nevertheless, we observe that AB-MS-GLMB is slightly more accurate than our method. During this period, all filters produce relatively accurate cardinality estimation, which is due to the high detection probability of targets.

For the remaining tracking time, AB-MS-GLMB localisation error significantly increases and the cardinality is underestimated as shown in Fig. 4. This behaviour is also observed in the MS-GLMB filter. It can be explained by the severely low detection probability and the fact that the detection probability fed to the filters is higher than the true value. These factors lead to early track termination (hence underestimated cardinality) and less accurate measurement to track assignments (hence increase in OSPA$^{(2)}$ localisation error). R-MS-GLMB and our method do not exhibit this behaviour due to their ability to update the detection probability and clutter rate on-the-fly. Nevertheless, R-MS-GLMB's track cardinality estimation is worse than ours (see Fig. 3). Overall, our method shows robust tracking performance over the entire tracking duration.

In Fig. 5, we observe that the average detection probability estimated by our filter and the R-MS-GLMB filter are similar for the entire tracking duration. The clutter rate is estimated more accurately than the detection probability. These results confirm ones observed in [13].

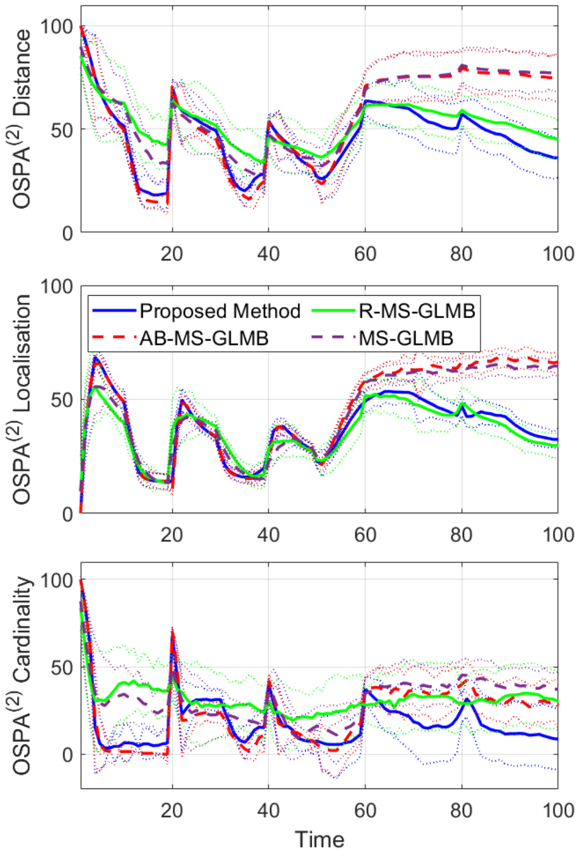

Fig. 3. OSPA$^{(2)}$ errors for different algorithms (unit is in m).

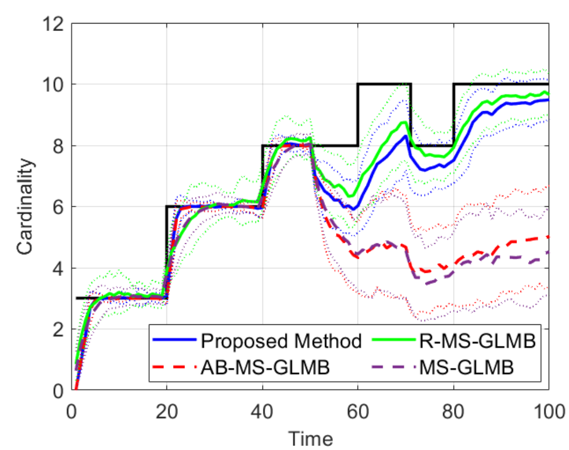

Fig. 4. Estimated cardinality.

V. Conclusion

We have proposed an adaptive filtering algorithm to track multiple targets in unknown clutter rate, detection probability, and birth statistics scenarios. By assuming linear Gaussian models, our algorithm allows closed-form analytic computation of the sampling distribution and the birth statistics. Experimental results have showed that our filter exhibits robust tracking performance in a challenging tracking scenario with significant variation in clutter rate and detection probability.

References

[1] R. Mahler, "CPHD and PHD filters for unknown backgrounds II: Multitarget filtering in dynamic clutter," in *Sensors and Systems for Space Applications III*, vol. 7330, 2009, p. 73300L.

[2] R. Mahler and A. El-Fallah, "CPHD filtering with unknown probability of detection," in *Signal Processing, Sensor Fusion, and Target Recognition XIX*, vol. 7697, 2010, p. 76970F.

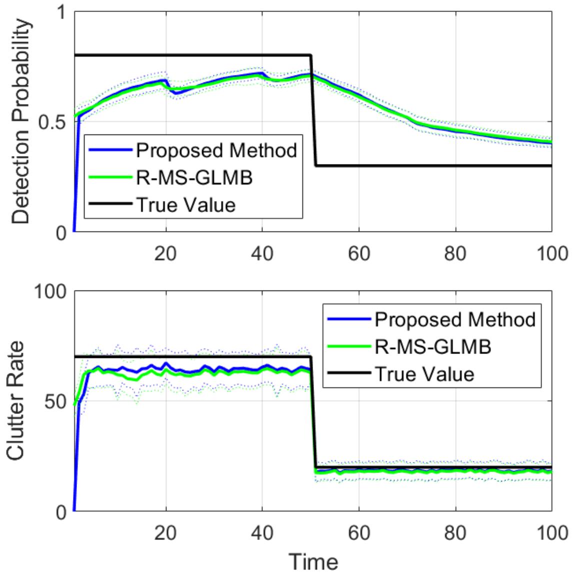

Fig. 5. Estimated average detection probability and clutter rate (for one sensor, the same behaviour observed for other sensors).

[3] R. Mahler, B.-T. Vo, and B.-N. Vo, "CPHD filtering with unknown clutter rate and detection profile," *IEEE Trans. Signal Process.*, vol. 59, no. 8, pp. 3497–3513, 2011.

[4] B.-T. Vo, B.-N. Vo, R. Hoseinnezhad, and R. P. S. Mahler, "Robust multi-Bernoulli filtering," *IEEE J. Sel. Topics Signal Process.*, vol. 7, no. 3, pp. 399–409, 2013.

[5] D. Y. Kim, "Visual multiple-object tracking for unknown clutter rate," *IET Computer Vision*, vol. 12, no. 5, pp. 728–734, 2018.

[6] Y. G. Punchihewa, B.-T. Vo, B.-N. Vo, and D. Y. Kim, "Multiple object tracking in unknown backgrounds with labeled random finite sets," *IEEE Trans. Signal Process.*, vol. 66, no. 11, pp. 3040–3055, June 2018.

[7] C.-T. Do and H. Van Nguyen, "Tracking multiple targets from multistatic Doppler radar with unknown probability of detection," *Sensors*, vol. 19, no. 7, 2019.

[8] C.-T. Do, T. T. D. Nguyen, D. Moratuwage, C. Shim, and Y. D. Chung, "Multi-object tracking with an adaptive generalized labeled multi-Bernoulli filter," *Signal Processing*, vol. 196, p. 108532, 2022.

[9] M. Beard, B. T. Vo, B.-N. Vo, and S. Arulampalam, "A partially uniform target birth model for gaussian mixture PHD/CPHD filtering," *IEEE Trans. Aerosp. Electron. Syst.*, vol. 49, no. 4, pp. 2835–2844, 2013.

[10] S. Reuter, B.-T. Vo, B.-N. Vo, and K. Dietmayer, "The labeled multi-Bernoulli filter," *IEEE Trans. Signal Process.*, vol. 62, no. 12, pp. 3246–3260, 2014.

[11] S. Lin, B.-T. Vo, and S. E. Nordholm, "Measurement driven birth model for the generalized labeled multi-Bernoulli filter," in *Int. Conf. on Control, Automation and Information Sciences*, 2016, pp. 94–99.

[12] A. Trezza, D. J. Bucci, and P. K. Varshney, "Multi-sensor joint adaptive birth sampler for labeled random finite set tracking," *IEEE Trans. Signal Process.*, vol. 70, pp. 1010–1025, 2022.

[13] C.-T. Do, T. T. D. Nguyen, and H. V. Nguyen, "Robust multi-sensor generalized labeled multi-Bernoulli filter," *Signal Processing*, no. 192, pp. 1–12, 2022.

[14] B.-N. Vo, B.-T. Vo, and M. Beard, "Multi-sensor multi-object tracking with the generalized labeled multi-Bernoulli filter," *IEEE Trans. Signal Process.*, pp. 1–1, 2019.

[15] B.-T. Vo and B.-N. Vo, "Labeled random finite sets and multi-object conjugate priors," *IEEE Trans. Signal Process.*, vol. 61, no. 13, pp. 3460–3475, 2013.

[16] B.-N. Vo, B.-T. Vo, and D. Phung, "Labeled random finite sets and the Bayes multi-target tracking filter," *IEEE Trans. Signal Process.*, vol. 62, no. 24, pp. 6554–6567, 2014.

[17] B.-N. Vo, B.-T. Vo, and H. G. Hoang, "An efficient implementation of the generalized labeled multi-Bernoulli filter," *IEEE Trans. Signal Process.*, vol. 65, no. 8, pp. 1975–1987, 2017.

[18] R. Mahler, "Exact closed-form multitarget Bayes filters," *Sensors*, vol. 19, no. 12, 2019.

[19] M. Beard, B.-T. Vo, and B.-N. Vo, "A solution for large-scale multi-object tracking," *IEEE Trans. Signal Process.*, vol. 68, pp. 2754–2769, 2020.

[20] B.-N. Vo and B.-T. Vo, "A multi-scan labeled random finite set model for multi-object state estimation," *IEEE Trans. Signal Process.*, vol. 67, no. 19, pp. 4948–4963, Oct 2019.

[21] D. Moratuwage, B. N. Vo, B. T. Vo, and C. Shim, "Multi-scan multi-sensor multi-object state estimation," *arXiv e-prints*, p. arXiv:2205.15516, 2022.

[22] D. Y. Kim, B.-N. Vo, A. Thian, and Y. S. Choi, "A generalized labeled multi-Bernoulli tracker for time lapse cell migration," in *Int. Conf. on Control, Automation and Information Sciences*, 2017, pp. 20–25.

[23] W. J. Hadden *et al.*, "Stem cell migration and mechanotransduction on linear stiffness gradient hydrogels," *Proc. of the National Academy of Sciences*, vol. 114, no. 22, pp. 5647–5652, 2017.

[24] T. T. D. Nguyen, B.-N. Vo, B.-T. Vo, D. Y. Kim, and Y. S. Choi, "Tracking cells and their lineages via labeled random finite sets," *IEEE Trans. Signal Process.*, vol. 69, pp. 5611–5626, 2021.

[25] M. Beard, B.-T. Vo, B.-N. Vo, and S. Arulampalam, "Void probabilities and Cauchy-Schwarz divergence for generalized labeled multi-Bernoulli models," *IEEE Trans. Signal Process.*, vol. 65, no. 19, pp. 5047–5061, 2017.

[26] D. Moratuwage, M. Adams, and F. Inostroza, "δ-generalised labelled multi-Bernoulli simultaneous localisation and mapping," in *Int. Conf. on Control, Automation and Information Sciences*, 2018, pp. 175–182.

[27] ——, "δ-generalized labeled multi-Bernoulli simultaneous localization and mapping with an optimal kernel-based particle filtering approach," *Sensors*, vol. 19, no. 10, 2019.

[28] H. V. Nguyen, H. Rezatofighi, B.-N. Vo, and D. C. Ranasinghe, "Online UAV path planning for joint detection and tracking of multiple radio-tagged objects," *IEEE Trans. Signal Process.*, vol. 67, no. 20, pp. 5365–5379, 2019.

[29] S. Panicker, A. K. Gostar, A. Bab-Hadiashar, and R. Hoseinnezhad, "Tracking of targets of interest using labeled multi-Bernoulli filter with multi-sensor control," *Signal Processing*, vol. 171, p. 107451, 2020.

[30] D. Y. Kim, B.-N. Vo, B.-T. Vo, and M. Jeon, "A labeled random finite set online multi-object tracker for video data," *Pattern Recognition*, vol. 90, pp. 377 – 389, 2019.

[31] J. Ong, B.-T. Vo, B.-N. Vo, D. Y. Kim, and S. Nordholm, "A Bayesian filter for multi-view 3D multi-object tracking with occlusion handling," *IEEE Trans. Pattern Anal. Mach. Intell.*, pp. 1–1, 2020.

[32] T. Rathnayake, A. K. Gostar, R. Hoseinnezhad, and A. Bab-Hadiashar, "Labeled multi-Bernoulli track-before-detect for multi-target tracking in video," in *Int. Conf. on Information Fusion*, 2015, pp. 1353–1358.

[33] T. Rathnayake, A. Khodadadian Gostar, R. Hoseinnezhad, R. Tennakoon, and A. Bab-Hadiashar, "On-line visual tracking with occlusion handling," *Sensors*, vol. 20, no. 3, 2020.

[34] T. Rathnayake, R. Tennakoon, A. Khodadadian Gostar, A. Bab-Hadiashar, and R. Hoseinnezhad, "Information fusion for industrial mobile platform safety via track-before-detect labeled multi-Bernoulli filter," *Sensors*, vol. 19, no. 9, 2019.

[35] H. V. Nguyen, H. Rezatofighi, B.-N. Vo, and D. C. Ranasinghe, "Distributed multi-object tracking under limited field of view sensors," *IEEE Trans. Signal Process.*, vol. 69, pp. 5329–5344, 2021.

[36] D. Moratuwage, M. Adams, and L. Cament, "Space object tracking using a jump Markov system based δ-GLMB filter for space situational awareness," in *Advanced Maui Optical and Space Surveillance Technologies Conf.*, 2019.

[37] S. Quan, D. Ding, and N. Zhaodong, "Space debris tracking via generalized labeled multi-Bernoulli random finite sets," in *Int. Conf. on Signal Processing, Communications and Computing*, 2019, pp. 1–4.

[38] B. Wei and B. Nener, "Distributed space debris tracking with consensus labeled random finite set filtering," *Sensors*, vol. 18, no. 9, 2018.

[39] T. T. D. Nguyen, H. Rezatofighi, B.-N. Vo, B.-T. Vo, S. Savarese, and I. Reid, "How trustworthy are performance evaluations for basic vision tasks?" *arXiv e-prints*, p. arXiv:2008.03533, 2020.